Silicon Microstrip Detectors in High Luminosity Application

Hartmut F.-W. Sadrozinski
SCIPP, University of California Santa Cruz, Santa Cruz, CA 95064

Abstract

The development of silicon microstrip detectors for high luminosity application at the Large Hadron Collider (LHC) is described. The technical choices are most severely restricted by the anticipated radiation damage. A radiation-tolerant choice for the silicon tracker of the LHC detector ATLAS are sandwiches of single-sided detectors with n-strips in n-type bulk.

I. INTRODUCTION

The advent of high luminosity colliders requires special instrumentation in High Energy Physics [1-3]. A new problem at the hadron colliders are the increased radiation levels. This applies especially to semiconductor detectors, which, due to their relatively high cost and extremely good position resolution are commonly located close to the interaction region where the radiation levels are highest [4,5]. Thus it is not surprising that the silicon strip detectors developed for ATLAS SemiConductor Tracker (SCT) [5] differ from those developed for low-luminosity applications such as LEP [6] or for BaBar [7], where only ionizing radiation is present.

In this report, the basic functioning of silicon microstrips will be reviewed first, followed by discussion of radiation damage in silicon detectors. The design of the ATLAS SCT modules will be presented, and features highlighted which are specific to the operating conditions at the LHC. The projected performance of both irradiated and un-irradiated detectors will be detailed, based on beam test measurements. The consequences of very high operating voltages will be discussed.

II. BASICS OF SILICON MICROSTRIP DETECTORS

Silicon strip detectors [8,9] are made from nearly intrinsic bulk having both low-ohmic donor implants (the n-side), collecting electrons, and low-ohmic acceptor implants (the p-side), collecting holes. The n-side signal is mainly due to drifting electrons collected in ~8ns, (for the usual 300micron thickness and with bias above the depletion voltage). The p-side signal is mainly due to drifting holes with a collection time three times longer, due to their lower mobility. One side has a junction, the other is ohmic. The location of the junction depends on the type of the bulk: it is on the p-side in n-bulk and the n-side in p-bulk. Charge is collected only from the depleted region, which starts at the junction side when the bias voltage is raised from zero, and reaches the full thickness of the detector at the depletion voltage. Single-sided detectors have only one side divided into strips which are read out, double-sided detectors have both sides divided into read-out strips. Most (all?) silicon detectors are made of high-ohmic n-bulk with resistivity of about 5kΩ-cm, determined by a small fraction (10^{12} per cm^3) of donor atoms. The distance between strip centers, the pitch, is of the order of 50 microns, and the read-out electronics is directly wire-bonded to the strips and helps in the data compression of the large number of channels [10-12].

The original single-sided detectors had the p strips implanted in n-bulk and coupled directly to the read-out electronics. Later, AC-coupling was developed which decoupled the DC current and the biasing potential from the front-end electronics. This made the use of double-sided detectors feasible, which are an economical and low-mass technical choice [13].

III. RADIATION DAMAGE IN SILICON STRIP DETECTORS

Radiation damage increases the reverse bias current and the depletion voltage of the silicon detectors.

A. Surface Damage

Ionizing radiation deposits charges on the surface of silicon strip detectors, which change their electrical properties. The processing of the surface, and the existence of oxides or nitrides can be a factor in the extent and consequences of the damage. During irradiation with large dose rates, increased leakage currents were observed due to charge-up of the surface, which annealed out in less than an hour at room temperature [14,15]. These effects are difficult to quantify and we have dealt with them by performing a beam test at particle fluxes and operating temperatures anticipated for the LHC to be able to observe deteriorated performance (see Sec. V).

A more lasting damage to the surface is due to the accumulation of charges in the interface between the silicon oxides and the silicon bulk, where there is a lattice mismatch. The interface states are filled due to ionizing radiation and saturate after a total dose of the order of 100kRad [16]. The important detector parameters which can be influenced by the existence of these oxide charges are bias resistance, interstrip resistance and interstrip capacitance.

Polysilicon bias resistors are radiation hard [16], while those using an accumulation layer or the punch-through effect are changed drastically with radiation [17,18]. Moreover, the punch-through resistors introduce excess noise [18].

The interstrip resistance is crucial for the isolation of the strips, and has to be much larger than the biasing resistor and the input impedance of the amplifier. The isolation is a problem on the n-side (ohmic side) before radiation due to the existence of a conducting accumulation layer of electrons below the oxide charges, but can be cured by implanting p-material as isolation ("p-stops") [19]. After irradiation, when the bulk inverts [see below] and the junction is on the n-side, this problem vanishes.

0018-9499/98$10.00

The interstrip capacitance is the largest contributor to the parasitic capacitance responsible for amplifier noise. In the absence of free charges, it can be estimated fairly reliably from the geometry of the strip detector and is a function of the ratio strip width over strip pitch [20,21]. The existence of free charges on the n-side before inversion causes the capacitance to depend on the bias voltage and one reaches the minimum "geometrical" value only with large over-voltage.

Surface currents due to the oxide charges have been observed, but they are less important than the bulk currents for charged particle radiation [16,22,23].

B. Bulk Damage

The bulk is damaged mainly by displacement ["Non-ionizing Energy Loss" (NIEL)] [24], leading to an increase in the leakage current due to the creation of deep acceptor levels and a change in the depletion voltage due to the change in effective doping concentration.

1) Increase in Leakage Current

The leakage current is due to a thermal generation of electron-hole pairs [25]. It varies exponentially with the operating temperature. Radiation increases the leakage current i proportionally with the displacing fluence ϕ and the volume Vol

$$i = \alpha \cdot \phi \cdot Vol \qquad (1)$$

with $\alpha \approx 3*10^{-17}$A/cm for high energy protons after annealing [26]. A large part of the current seems process dependent, but anneals out very fast. The leakage current is the reason why AC coupled detectors are used, which block the current from the amplifier input. But it also causes stochastic noise in the amplifier, proportional to the square root of the product of leakage current and shaping time. The allowable current limit for fast shaping times is about one μA per strip.

Figure 1 shows a typical i-V curve after irradiation with high energy protons to a fluence of $2*10^{14}$ p/cm^2 [15]. The current above the depletion voltage of about 300V is not constant, which causes the generated heat in the detector to depend on the square of the bias voltage.

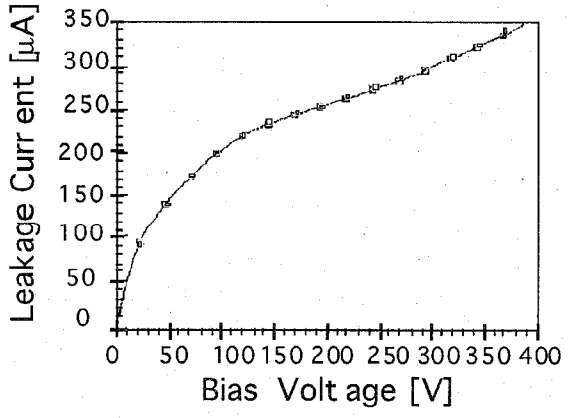

Figure 1: I-V characteristic of a detector irradiated to a fluence of $2*10^{14}$ p/cm^2 (Ref. 15).

2) Change in Depletion Voltage

The depletion voltage V_{dep} depends on the effective doping concentration N_{eff} and the square of the detector thickness d:

$$V_{dep} = \frac{e \cdot |N_{eff}| \cdot d^2}{2 \cdot \varepsilon} \qquad (2)$$

Thus a radiation induced change in the doping concentration causes a change in the depletion voltage [27]. The effective doping concentration is changed in two ways: an exponential donor removal and a linear acceptor creation, and both make the bulk more p-type [Fig. 2]

$$N_{eff} = N_0 e^{-c\phi} + \beta\phi \qquad (3)$$

At a certain fluence, about $\phi = 1*10^{13}$p/cm^2 in Fig. 2, the remaining donors are balanced by the newly created acceptors and the detector is intrinsic with zero depletion voltage. For larger fluences, the acceptors dominate and the detector is inverted, *i.e.* p-type, and the detector is said to have undergone "type inversion". For large fluences, the depletion voltage increases linearly with fluence, and is independent of the pre-rad value.

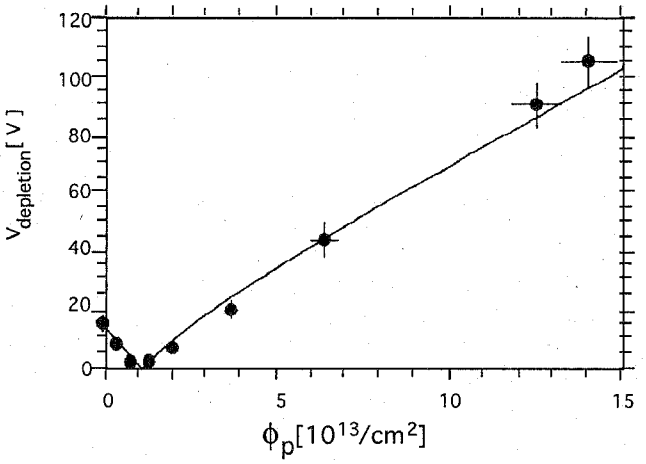

Figure 2: Depletion voltage change due to radiation damage in a 170μm thick n-bulk photo diode as a function of proton fluence ϕ_p. For 300μm thick detectors, the depletion voltages would be about three times as high (Ref. 27).

3) Annealing

The radiation induced changes in detector properties are initially not stable, but exhibit strong annealing, which is temperature dependent [28-30]. This means that the increased leakage currents and the modified doping concentration change even after the irradiation has finished. For example, at room temperature, the leakage currents decrease by about a factor of two in a few weeks. The annealing of the doping concentration is more complicated: there are three different effects with different time constants: there is first a constant term; then a short term annealing governed by τ_S, which is beneficial because it reduces the depletion voltage; and a long-term reverse- ("anti") annealing effect due to the release of meta-stable acceptors, which increases the depletion voltage with a characteristic time τ_L.

In good approximation for the fluences at the LHC, the three components, stable, short-term, and long-term annealed, respectively, are proportional to the fluence ϕ

$$V_{dep} = \phi[v_z + v_s e^{-t/\tau_s} + v_a(1 - e^{-t/\tau_L})] \quad . \qquad (4)$$

Both annealing times are exponential functions of the temperature; the long annealing time τ_L is about 200 times longer than the short anneal time τ_S. After a fluence of $\phi = 2*10^{14}$p/cm^2, a typical fluence for 10 years of LHC operation [31], the constant term in the depletion voltage is about 200V, the short-term annealing term is about 600V and the reverse annealing term is also 600V [28]. Thus, depending on the operating temperature, the depletion voltage can vary between 200V and 800V. This is shown in Fig. 3, where the depletion voltage for different detectors irradiated to the same fluence of about $5*10^{13}$p/cm^2, but annealed out at different temperatures is shown: the detectors operated at elevated temperatures are reverse-annealed out completely to about 230V, while the detectors operated at 0°C or below are still in the first phase of short-term annealing.

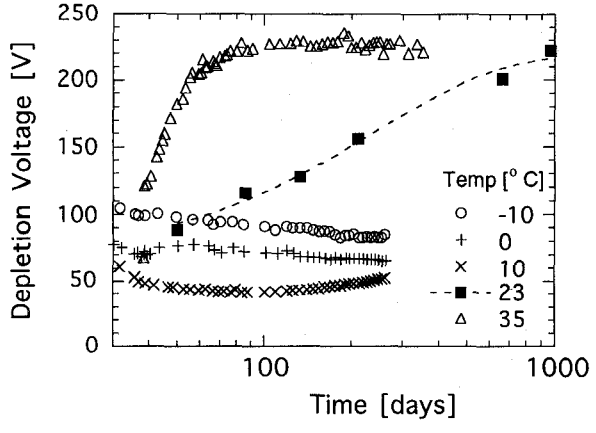

Figure 3: Temperature dependence of the annealing of the depletion voltage for photo diodes irradiated with about $5*10^{13}$p/cm^2. The detector at 23°C was kept at -20°C until day 30 (Ref. 28).

IV. CONSEQUENCES FOR THE OPERATION OF SILICON STRIP DETECTORS

Radiation damage influences the performance of the detectors (signal, noise, position resolution) and the operating condition (bias voltage and heat generation).

A. Charge Collection on a single Strip

For the binary readout scheme which has been adopted by ATLAS [10-12], the efficiency is determined by the charge collection on a single strip. The signal collection before and after irradiation has been studied [15,32,33] and depends primarily on the applied bias voltage [34]. First there is signal loss due to charge trapping. The loss of charge due to trapping is of the order 15% at the highest LHC fluences considered [35]. The total signal charge is proportional to the width of the depleted region x, which depends on the ratio of the bias voltage to the depletion voltage

$$x = d*\sqrt{\frac{V_{bias}}{V_{dep}}} \quad , \quad V_{bias} < V_{dep}$$
$$x = d \quad , \quad V_{bias} \geq V_{dep} \qquad (5)$$

where d is the detector thickness. This functional dependence of the collected charge on the square root of the depletion voltage is correct for the junction side both before and after irradiation. Fig. 4 shows the n-side signal after heavy irradiation for two different fluences [15].

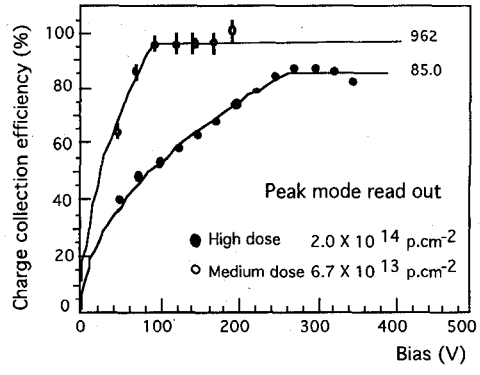

Figure 4: Total charge collected on an irradiated n-on-n detector after irradiation to $0.7*10^{14}$ and $2*10^{14}$p/cm^2 (Ref. 15).

Biased below depletion, the signal collection on one strip depends on whether the collection happens on the junction side or on the ohmic side. On the junction side, the signal charge is collected on one or two strips. On the ohmic side, the charge is collected on many strips. Consequently, the efficiency for detecting tracks on the ohmic side is reduced if operated below depletion . This is shown in Fig. 5, where the efficiency of detecting min. ion. tracks is shown for the two sides of a double-sided detector, both before and after irradiation [32]. The signal collection after irradiation is well measured, although the charge sharing depends somewhat on the strip width. Before irradiation (Fig. 5a), the depletion voltage is between 50V and 100V and the detectors can easily be biased above depletion. As expected, the ohmic (n-) side has a much more abrupt voltage dependence than the junction (p-) side.

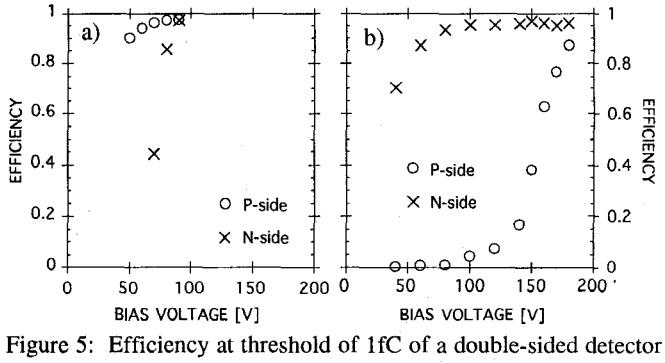

Figure 5: Efficiency at threshold of 1fC of a double-sided detector with 50μm pitch a) un-irradiated with a depletion voltage of 77V, b) irradiated with depletion voltage 190V (Ref. 32).

At a fluence of about 10^{13}p/cm^2 (~1/20 of the total life time for the ATLAS SCT), the bulk inverts from n-type to

p-type. The junction moves to the n-side. As before irradiation, the charge collection on the junction side is efficient even below depletion (Fig. 5b). The p-side becomes the ohmic side, and below depletion, the generated charge is collected on several strips. Hence, for irradiated detectors, operation close to depletion is required for the p-side, while operation below depletion is possible for the n-side. The n-side exhibits good efficiency >95% when biased at 50% of depletion voltage, while the p-side shows good efficiency only when biased close to the depletion voltage (Fig. 5b).

B. Operating Voltage

Because read-out on the junction side allows the detector to be operated under-depleted, n-on-n single-sided detectors function, after inversion, almost as well as before radiation up to much larger fluences than originally anticipated. If the system is designed for a maximum bias voltage of 300V - which by now has been routinely used in several beam tests (see Sec. V below), - it will work with 95% efficiency even if the depletion voltage turns out to be 600V, due to increased luminosity, radiation accidents or possible warm-up. If p-side detectors are used in high radiation conditions, they will require larger operating voltages, expected to be a factor 1.5 to 2 higher. Consequently, the entire SCT system, detectors and their coupling capacitors, power supplies, bypassing, cables etc., has to be designed to the largest depletion voltage foreseeable, because changes in the conditions which increase the maximum depletion voltage beyond the anticipated goal strongly reduce the p-side performance. In addition, the increased heat load for higher bias operation has to be planned for: increasing the bias voltage from 300 to 500V increases the heat load by at least a factor 2, which has to be dealt with appropriate cooling (see Sec. VI).

The fact that n-on-n detectors can be operated under-depleted can be exploited in pixel detectors, which could be operated at a reasonably low bias even in the case of a large depletion voltage [36-38]. We have irradiated a single-sided n-on-n detector to 10^{15} p/cm^2, where the depletion voltage is about 2000V, and extracted at 180V bias the pulse height, amounting to 20% of the pre-rad value (Fig. 6). With the very low pixel capacitance, this small signal charge gives sufficient signal-to-noise for efficient track detection very close to the interaction point.

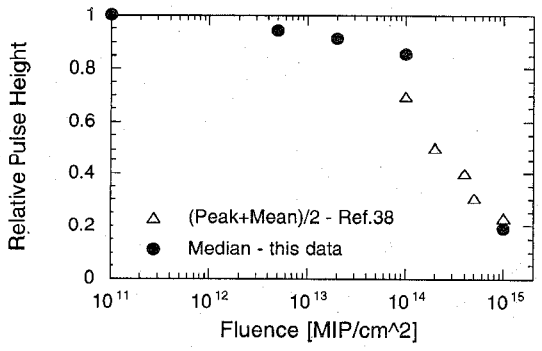

Figure 6: Relative pulse height of n n-on-n detector at 180V bias (Ref. 37).

Several attempt have been made to reduce the ultimate depletion voltage by using different bulk materials. One idea was to use p-material, with n-implants. It has the advantage that there is no inversion during the detector life time due to radiation damage: the junction stays on the n-side, and the quality control of the detectors is simplified. Unfortunately, there is much less experience with p-bulk processing and more importantly, the radiation damage constants for p-bulk are not much different than for n-bulk [39,40]. In addition, for the same resistivity, the depletion voltage of p-bulk detectors is a factor three higher than of n-bulk detectors due to the lower mobility of the holes, which are the majority carriers in the p-bulk. Thus the ultimate depletion voltage will be higher than for n-bulk detectors. Another idea was to use lower resistivity n-bulk material for the detector, which increases the initial pre-rad depletion voltage and shifts the inversion point to higher fluences [41]. Given that the depletion voltage at very large fluences is determined by acceptor creation and not by the removal of donors, the ultimate depletion voltage is the same for both high- and low-ohmic material [42].

There is no long-term experience operating heavily irradiated detectors with short shaping times. In laboratory and beam tests, the n-side on irradiated detectors have shown somewhat reduced capacitance and noise with fast shaping front-end electronics (FEE) due to the fact that they have become the junction side. Laboratory measurements on p-side detectors have shown, below depletion, increased inter-strip capacitance and increased noise after radiation [21, 43].

C. Single-sided vs. double-sided Detectors

Given that the n-side have superior radiation resistance, the use of the p-side is less advantageous. Indeed, the ATLAS SCT will build sandwiches of two single-sided n-on-n detectors, glued back-to-back, to make a double-sided module. This way the read-out strips and the front-end electronics are at ground, with many advantages for the operation and safety of the detectors at high depletion voltages and the stability of the FEE. For example, the largest voltage across the coupling capacitors is less than one volt, reducing the stress on the oxide. Gluing on either the junction or ohmic side has been shown not to deteriorate the performance of the detectors as long as the detectors were passivated [44].

D. Operating Temperature

In order to conserve power, and for safe operation, the depletion voltage should be kept as low as possible. Over the lifetime of the detectors at LHC, the detectors will be subjected to fluences in excess of $2*10^{14}$p/cm^2. The depletion voltage will change from the initial pre-rad value of about 50V to zero to a final value which depends both on the fluence and the operating temperature. Type inversion (see above) occurs at a fluence of about 10^{13}p/cm^2 , i.e., after less than one year at full LHC luminosity. Given that the damage constants are proportional to the fluence received by the detector, the only additional parameter which controls the depletion voltage is the operating temperature. It has to be kept low to prevent the reverse annealing, but to allow the

short-term annealing to take place during the lifetime t of the detector:

$$\tau_S << t << \tau_L \quad (6)$$

For the life time of the LHC detectors of about t = 10 years, this corresponds to an operating temperature between -5 and -10°C [30]. Access scenarios which result in warm-up of the irradiated detectors have to be evaluated carefully. For example, warming up the detectors every year for 7 days from -10° to +20°C [5], instead of keeping the operating temperature constant at -10°C, will increase the depletion voltage by 30% .

As mentioned before, the leakage current is a noise source. Short shaping times are required, in addition to the low temperature to minimize the current [10]. The leakage current produces heat, which has to be removed. Due to the exponential temperature dependence of the leakage current, the self-heating has to be controlled carefully in order to avoid thermal run-away [45], which puts stringent requirements on the cooling system (see Sec. VI).

V. DESIGN AND PERFORMANCE OF THE ATLAS SCT DETECTORS

Uncertainties in predicting the dose and operating temperature require that the detectors be designed with "head room", *i.e.*, enough margin in performance to minimize degradation due to unforeseen conditions. Although there has been many years of experience with silicon detectors for example at LEP [6], detectors have been used in high rate and high radiation environment only in the SVX at the FNAL Collider [18] and the LPS at HERA [14].

A certain amount of conservatism is applied to the detector design because one extrapolates the finding of short-term R&D to operation for 10 years in ATLAS. The prediction [5,31] for the depletion voltage for the innermost SCT layer at 30cm radius varies from 150V to 250V, depending on the assumptions. In the forward region, the expected values are between 300V and 500V. There is considerable uncertainty in the depletion voltage prediction, depending on assumption made for the radiation history and the operating temperature of the detectors. Thus, for the ATLAS SCT, the detector specifications call for 50% higher fluence than expected and for an access/warm-up scenario which increases the depletion voltage by 30% above the minimum [5].

A. Design of the ATLAS SCT Detectors

The prospect that the detector can be operated efficiently at a bias voltage below 300V for the predictable life time at the LHC and that it can function with only slightly reduced performance at the same bias voltage even in the case that the depletion voltage is twice as large, has led to using single-sided n-bulk detectors with n-side read-out and polysilicon biasing.

Two layers of detectors are glued to a highly conductive base plate to make a double-sided sandwich (Fig. 7). Two 6cmx6cm detectors are bonded together to make 12cm read-out strips and are then glued back-to-back with another 12cm long pair, making a 40mrad stereo angle. The electronic readout (hybrid) is straddling the center of the module, to minimize the noise contribution from the strip resistance [43]. Good thermal properties are guarantied with a "heat spreader" made of thermally highly conductive pyrolytic graphite (PG). The pitch of the detectors is 80μm, with narrow (≈ 16μm wide) implants to minimize the interstrip capacitance [20,21].

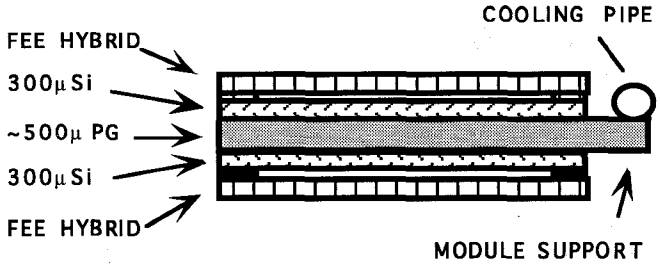

Figure 7: Schematic cross section through the ATLAS module: a Silicon-PG-Silicon sandwich.

B. Performance of the ATLAS SCT Detectors

A series of beam tests have been performed with 12cm long modules of single-sided n-on-n silicon detectors and fast FEE [46]. Identical modules were tested in 1996 in the H8 test beam at CERN, with one of them irradiated with 55MeV protons to a fluence in excess of 10^{14}p/cm^2, such that the depletion voltage was 290V, as determined with C-V measurements. The detectors were operated cold (at about -10°C) and rotated relative to the beam in a magnetic field of 1.56T to investigate the performance for tracks with crossing angles as expected in the ATLAS detector [5]. The performance is expressed in tracking efficiency, noise occupancy and position resolution. The noise occupancy was far below 10^{-3} for 1fC threshold. The efficiency of n-on-n detectors is high in the un-irradiated detector when over-depleted (at bias >100V), and in the irradiated detector at 150V which is one half the depletion voltage (Fig. 8). Thus even in heavily irradiated detectors, the performance is recovered by raising the bias voltage.

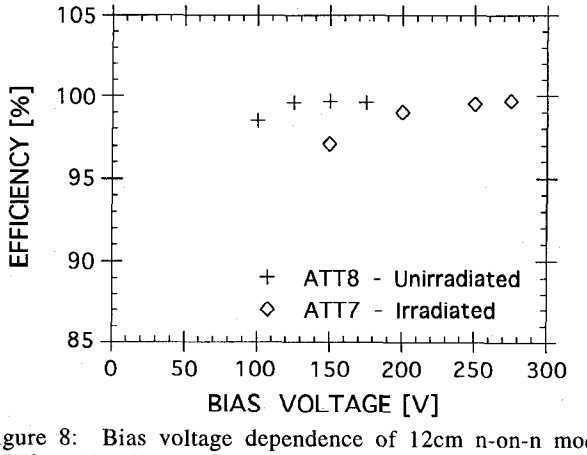

Figure 8: Bias voltage dependence of 12cm n-on-n modules ATT8 and irradiated ATT7 (depletion voltage 290V): efficiency at 1fC threshold (Ref. 46).

In the ATLAS experiment, tracks will cross the detector planes with angles up to $\pm 15^{o}$ due to the Lorentz force and the finite width of the detectors, which will be tilted by an angle of about $+10^{o}$. This effect was explored by rotating the detectors in the magnetic field: the efficiency is independent of rotation angle for the required range of $\pm 15^{o}$ relative to the anticipated tilt angle (Fig. 9). When biased at half the depletion voltage (150V, Fig. 9) , the efficiency of the irradiated detector ATT7 is still 95% at 1.0fC threshold. It turns out that biased at the full depletion voltage the efficiency is high even at a threshold of 1.2fC, 20% higher than the threshold required for noise suppression [43].

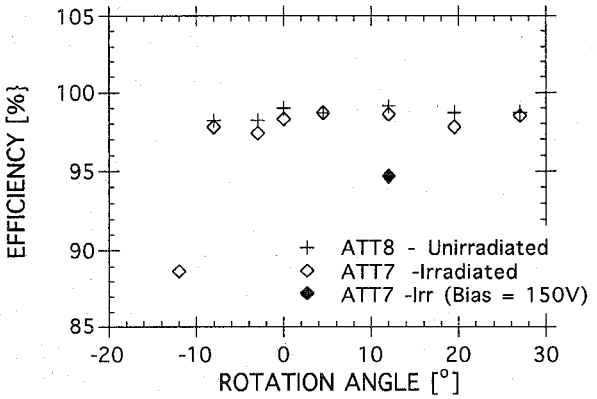

Figure 9: Rotation angle dependence in a 1.56T magnetic field with bias at 250V & 150V (ATT7) and 125V (ATT8): efficiency at 1fC (Ref. 46).

The position resolution (Fig. 10) of the irradiated detector is identical to the un-irradiated one. It is constant as a function of rotation angle and close to the expected value of pitch/$\sqrt{12}$. At half the depletion voltage (150V), the position resolution for ATT7 is the same as at full depletion.

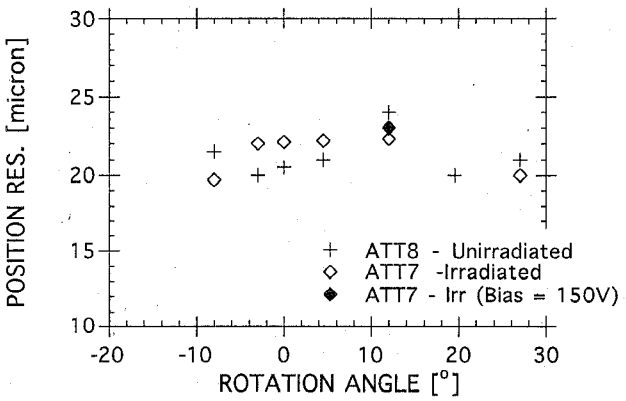

Figure 10: Rotation angle dependence in a 1.56T magnetic field with bias at 250V & 150V (ATT7) and 125V (ATT8): position resolution at 1fC (Ref. 46).

In general, the irradiated detector is almost indistinguishable from the un-irradiated, except that the operating voltage is twice as high and the leakage currents are 1000 times larger.

As mentioned in Sec. III, short-term radiation effects can effectively be understood only under realistic operating conditions. For part of the runs, the intensity of the test beam was increased to the instantaneous flux expected for operation at the LHC. During this high flux operation, no change in efficiency was observed neither for the un-irradiated nor for the inverted module (Fig. 11).

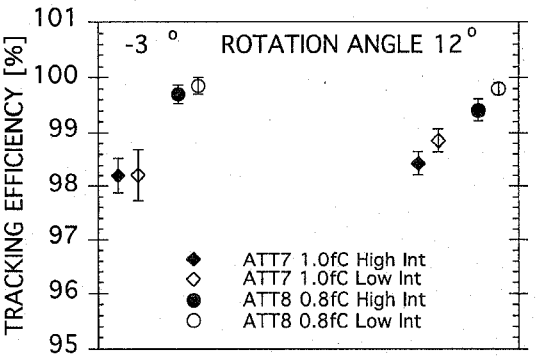

Figure 11: Efficiency for both irradiated (ATT7) and un-irradiated (ATT8) module during high and low intensity running for two rotation angles (Ref. 46).

The n-on-n detectors show an efficiency which is almost unchanged when the threshold is increased from 1.0fC to 1.2fC. This is due to the high signal-to-noise ratio of about S/N = 15. After radiation damage, the head room can be used to operate under-depleted, if warranted by unforeseen run conditions. At half depletion voltage, the resolution is unchanged and the efficiency is still 95%.

VI. OPERATIONS OF THE SCT

The effects of radiation damage have to be mitigated by cooling. Both the leakage current and the reverse annealing in the depletion voltage are reduced at low temperatures. But even at operating temperatures of -10^{o}C, the heat conduction in 300μm thick wafers not good enough to prevent local heating of the detectors. This can lead to thermal run-away [45, 47]. The thermal properties of the silicon modules can be vastly improved with the introduction of a "heat spreader", a thin layer of highly thermally conductive material sandwiched between two single-sided detectors, which effectively brings the cooling pipe close to the self-heated detector (Fig. 7). The ATLAS SCT modules will use a plane of pyrolytic graphite (PG) which has a heat conductivity κ close to CVD diamond. As a proof of principle both thermal [48] and electrical proto types [49] of the silicon-PG-silicon sandwich were built to investigate the thermal and electrical properties of the PG material, and they worked as expected.

A simulation [50,51] of the temperature distribution across a 12cmx6cm module was performed as a function of the internal heating for both a single wafer module and the Si-PG sandwich. It shows that the Si-PG sandwich allows a factor of at least 5 in the acceptable internal heating before thermal run-away. The temperature profile across a 6cmx12cm module, was both simulated and measured, for a heat input of 3mW per electronics channel and internal heating of about $100\mu W/mm^3$ and shows a maximum

temperature difference across the wafers of about three degrees. This heat production corresponds to a strip current of close to 1μA at 300V mentioned above as limit per channel for the electronics noise.

The dependence of the detector temperature on the generated heat is shown in Fig. 12 for different heat conductivity κ of the heat spreader (PG700 has κ=700 [W/m-^{o}K], Si has κ=130 [W/m-^{o}K]). This is done for a specific ATLAS module minimizing the amount of PG used [50].

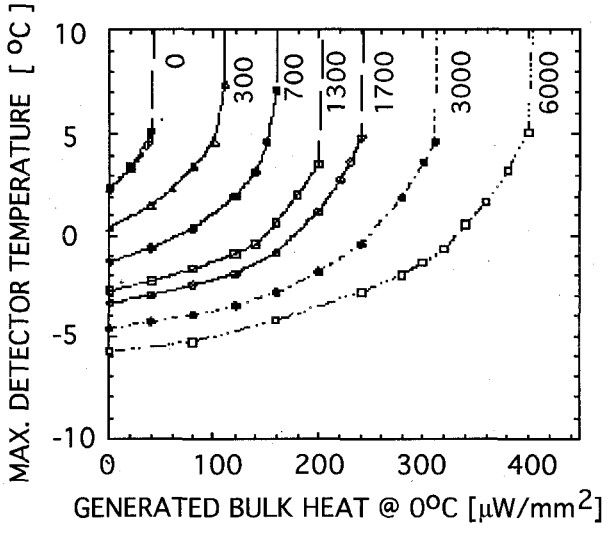

Figure 12: Simulation of the maximal wafer temperature on a silicon detector with one edge cooled to -10°C as a function of the internal heating. The parameter varied is the heat conductivity, as indicated on the curves (Ref. 51).

The advantage of the highly conductive material is seen, allowing much larger heat generation without thermal runaway. This is shown in Fig. 13, where the heat generation at thermal run-away is shown for each κ value of Fig. 12. An approximate square root dependence is seen, typical for an uniform heating. In addition, two horizontal lines represent typical heat generation of an irradiated detector at operating voltage 300V and 500V, respectively, increased by a safety factor 2.

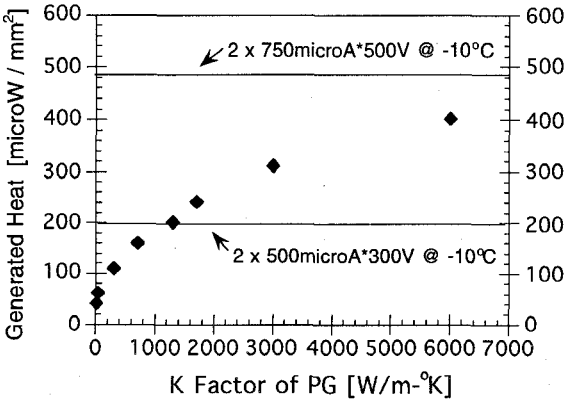

Figure 13: Heat generation at which thermal run-away occurs as a function of heat conductivity K of the PG heat spreader (Ref. 51).

While the heat generated at 300V bias can be conducted away with PG1300, the heat generated at 500V can't be conducted away with the PG thickness chosen, even for unphysical large values for the heat conductivity. That means that the thickness of the PG heat spreader has to be increased, adding to the critical materials budget. Increased waste heat is one argument against high voltage operation of silicon detectors, and argues for using n-side detectors with which the heat load and thus the material can be minimized by operating under-depleted.

VII. CONCLUSIONS

For the ATLAS silicon tracker, a sandwich of single-sided n-on-n detectors is presented as the base line, because their superior performance after heavy radiation damage has been proven over the last years. They exhibit good signal-to-noise ratio, even when operated under-depleted after radiation induced inversion. The alternative, p-side detectors, has been shown to require full depletion on the p-side and thus higher operating voltage. This higher operating voltage leads increased risk and material. On the other hand, p-side detectors appear to be significant cheaper.

In several beam tests, fully instrumented modules have been operated, some of them irradiated with realistic LHC fluences. The results confirm that the single-sided n-on-n detector affords the performance head room required for the high radiation environment of ATLAS and the uncertainty in predicting the operating conditions. With n-on-n detectors, the ATLAS SCT will be able to survive either higher radiation levels than anticipated or unexpected scenario's of warming up of the detectors, and will be able to profit from a more optimistic luminosity scenario.

VIII. ACKNOWLEDGMENTS

The contributions of many people the development of silicon detectors for high luminosity application have been acknowledged in the references. I would like to thank the staff of the SCIPP Microelectronics laboratory for their excellent work, and Taka Kondo for his simulations. This work has been supported by the US Department of Energy.

IX. REFERENCES

[1] A Toroidal LHC Apparatus ATLAS Technical Proposal, CERN/LHCC/94-43.

[2] The Compact Muon Solenoid CMS Technical Proposal, CERN/LHCC/94-38.

[3] A Large Ion Collider Experiment ALICE Letter of Intent, CERN/LHCC/93-16.

[4] H. F.-W. Sadrozinski, A. Seiden and A. Weinstein, *Nucl. Instr. Meth.* A277, 92 (1989).

[5] ATLAS Inner Detector Technical Design Report, CERN/LHCC/97-16/17.

[6] P. Collins, *Nucl. Instr. Meth.* A383, 1 (1996).

[7] R. P. Johnson, *Nucl. Instr. Meth.* A383, 7 (1996).

[8] M. Turala, Silicon Microstrip Detectors, DPF Conference 1985, Eugene, OR.

[9] A. Litke and A. Schwarz, The Silicon Microstrip Detector, *Scientific American* 272, 56 (May 1995).

[10] D. Dorfan, *Nucl. Instr. Meth.* A342, 143 (1994).

[11] A. Ciocio *et al.*, A Binary Readout System for Silicon Strip Detectors at the LHC, Presentation at the LHC Electronics Workshop, Lisbon, Portugal, Sept. 12, 1995.

[12] W. Dabrowski, *Nucl. Instr. Meth.* A383, 179 (1996).

[13] T. Ohsugi *et al.*, *Nucl. Instr. Meth.* A342, 16 (1994).

[14] E. Barberis *et al*, *Nucl. Instr. Meth.* A364, 507 (1995). (http://scipp.ucsc.edu/groups/silicon/papers/LPS.elec.6.ps), and Erratum: *Nucl. Instr. Meth.* A386, 535 (1997).

[15] P. Allport et *al.*, ATLAS Radiation Damage Study on Single- and Double-sided Silicon Strip Detectors, VERTEX '97.

[16] D. Pitzl *et al.*, *Nucl. Phys. B (Proc. Sup.)* 23A, 340 (1991).

[17] N. Bacchetta *et al., Nucl. Instr. Meth.* A342, 39 (1994).

[18] P. Azzi *et al.*, *Nucl. Instr. Meth.* A383, 155 (1996).

[19] R. Weaton, *Nucl. Instr. Meth.* A342, 126 (1994).

[20] R. Sonnenblick *et al.*, *Nucl. Instr. Meth.* A310, 189 (1991).

[21] E. Barberis *et al.*, *Nucl. Instr. Meth.* A342, 90 (1994).

[22] R. Wunstorf *et al., Nucl. Instr. Meth.* A377, 290 (1996).

[23] T. Ohsugi *et al.*, *Nucl. Instr. Meth.* A383, 166 (1996).

[24] A. Van Ginneken, Non-ionizing Energy Deposition in Silicon for Radiation Damage Studies, Fermilab Preprint FN522 (1989).

[25] E, Borchi, M. Bruzzi and M. S. Mazzoni, *Nucl. Instr. Meth.* A310, 273 (1991).

[26] E. Barberis *et al.*, *Nucl. Instr. Meth.* A326, 373 (1993).

[27] D. Pitzl *et al.*, *Nucl. Instr. Meth.* A311, 98 (1992).

[28] H. Ziock *et al.*, *Nucl. Instr. Meth.* A342, 96 (1994) (http://scipp.ucsc.edu/~hartmut/Hiro.mod.ps).

[29] E. Frettwurst *et al.*, *Nucl. Instr. Meth.* A342, 119 (1994).

[30] J. Matthews *et al., Nucl. Instr. Meth.* A381, 338 (1996).

[31] G. W. Gorfine, Studies of Radiation Levels in the LHC and of Radiation Damage to Silicon Detectors, U. of Melbourne PhD Thesis, 1994.

[32] T. Dubbs *et al.*, *Nucl. Instr. Meth.* A383, 174 (1996), http://scipp.ucsc.edu/groups/silicon/preprints/hirosh.ps.

[33] Y. Unno *et al.*, *IEEE Trans. Nucl. Sci.* 43, 1175 (1996), (http://arkhp1.kek.jp/~unno/notes/IEEE95paper5.ps).

[34] J. Leslie, A. Seiden and Y. Unno, *IEEE Trans. Nucl. Sci.* 40, 557 (1993), (http://scipp.ucsc.edu/~hartmut/ATLAS/SIGSIM).

[35] C. Leroy *et al.*, Study of Charge Collection and Noise in Non-irradiated and Irradiated Silicon Detectors, CERN-ECP/96-05.

[36] I. Abt *et al.*, *IEEE Trans. Nucl. Sci.* 43, 1113 (1996).

[37] A. Gomez *et al.*, Pulse Height of an n-side Silicon Microstrip Detector after Proton Irradiation with a Fluence of $1*10^{15}$p/cm^2, SCIPP 96/42, IEEE N.S. Symposium 1997, Nov 1997, Albuquerque, NM, (http://scipp.ucsc.edu/~hartmut/LBL_Irr.paper.ps).

[38] R. Horisberger *et al.*, presented at the 7th Pisa Meeting, Elba, May 1997.

[39] G. N. Taylor *et al.*, *Nucl. Instr. Meth.* A383, 144 (1996).

[40] S. Terada *et al.*, *Nucl. Instr. Meth.* A383, 159 (1996).

[41] P. Giubellino *et al*, *Nucl. Instr. Meth.* A315, 156 (1992).

[42] The rate of donor removal has been disputed: see: B. C. MacEvoy, Imperial College PhD thesis, RAL-TH-97-003 (1997), and talks at this IEEE meeting.

[43] T. Dubbs *et al.*, *IEEE Trans. Nucl. Sci.* 43, 1119 (1996), (http://scipp.ucsc.edu/groups/silicon/preprints/IEEE95_noise.ps).

[44] O. Runolfson, *Nucl. Instr. Meth.* A383, 223 (1996)

[45] W. O. Miller *et al.*, Thermal Run-away in Silicon Strip Detectors, SCIPP 94/43.

[46] F. Albiol *et al.*, Performance of the ATLAS Silicon Strip Detector Modules, SCIPP 96/49 to be publ. in Nucl. Instrum. Methods, and references therein, (http://scipp.ucsc.edu/~hartmut/H8_96.ps).

[47] T. Kohriki *et al.*, *IEEE Trans. Nucl. Sci.* 43, 1200 (1996).

[48] W. O. Miller *et al., IEEE Trans. Nucl. Sci.* 44, 743 (1997), (http://scipp.ucsc.edu/~hartmut/spgs.ieee.ps).

[49] Y. Unno *et al.*, Evaluation of the p-stop structures in the n-side of the n-on-n silicon strip detector, IEEE N.S. Symposium 1997, Nov 1997, Albuquerque, NM.

[50] T. Kondo *et al.*, Thermal Simulation of ATLAS Barrel SCT Modules-II, KEK preprint dated 7/27/97.

[51] T. Kondo. private communication.